MedChemComm

Accepted Manuscript

This article can be cited before page numbers have been issued, to do this please use: C. Chough, S. Lee, M. Joung, J. Lee, J. H. Kim and B. M. Kim, *Med. Chem. Commun.*, 2018, DOI: 10.1039/C7MD00568G.

ROYAL SOCIETY OF CHEMISTRY

rsc.li/medchemcomm

View Article Online
DOI: 10.1039/C7MD00568G

Journal Name

ARTICLE

Design, synthesis and evaluation of (*R*)-3-(7-(*methyl(7H*-pyrrolo[2,3-*d*]pyrimidin-4-yl)amino)-5-azaspiro[2.4]heptan-5-yl)-3-oxopropanenitrile as a JAK1-selective inhibitor

Received 00th January 20xx,
Accepted 00th January 20xx

DOI: 10.1039/x0xx00000x

www.rsc.org/

Chieyeon Chough,[a,†] Sunmin Lee,[b,†] Misuk Joung,[b] Jaemin Lee,[b] Jong Hoon Kim[c] and B. Moon Kim[a,*]

Based on (*R*)-*N*-methyl-*N*-(5-azaspiro[2.4]heptan-7-yl)-7*H*-pyrrolo[2,3-*d*]pyrimidin-4-amine as a core scaffold, we identified (*R*)-3-(7-(methyl(7*H*-pyrrolo[2,3-*d*]pyrimidin-4-yl)amino)-5-azaspiro[2.4]heptan-5-yl)-3-oxopropanenitrile [**(*R*)-6c**] as a JAK1 selective inhibitor. The structural design was based on the combination of tofacitinib's 7-deazapurine and 5-azaspiro[2.4]heptan-7-amine. Compound **(*R*)-6c** exhibited 8.5 nM IC_{50} on JAK1 with a selectivity index of 48 over JAK2. To optimize **(*R*)-6c** as a lead compound, we performed *in vitro* ADME, hERG, kinase profiling, and pharmacokinetic tests. Mouse and rat *in vivo* studies verified that **(*R*)-6c** exhibited desired efficacies on CIA and AIA models.

Introduction

Rheumatoid arthritis (RA) is an autoimmune disease that affects approximately 1~2% of the worldwide population.[1,2] Considerable work has been conducted in search of therapeutic targets[3-5] and recently emerging molecular targets like cytokines[6,7], G-protein coupled receptors[8], and kinases[9,10] have surfaced. Therapeutic agents against these targets are categorized as disease-modifying antirheumatic drugs (DMARDs).[11] The most commonly used drugs include conventional synthetic DMARDs, such as methotrexate, sulfasalazine, leflunomide, and so on.[12] However, they cannot be used for long-term treatment due to low therapeutic response and severe side effects. To overcome such limitations, researchers have developed biological DMARDs[13] like etanercept, infliximab, and adalimumab. Although they exhibit higher efficacies than the synthetic ones, their applications also have several drawbacks due to high cost, efficacy limitation on single administration,[14] limited intravenous (i.v.) administration accessibility,[15] and so on.

To meet the unmet medical needs in RA, many researchers have concentrated efforts on developing new synthetic DMARDs equipped with high efficacy, low cost, and a convenient administration route. As a result, Janus kinase (JAK)/signal transducer and activator of transcription (STAT) signal pathway has been identified as one of new therapeutic targets. JAK kinases had first been isolated in 1989[16] and their roles were discovered in 1994.[17] Factors involved in the JAK-STAT signaling like the cytokines, receptors, STATs, and JAKs are related to many autoimmune diseases including rheumatoid arthritis, psoriasis, myelofibrosis, Crohn's disease, and ulcerative colitis. JAK3, out of four isotypes, has received the most attention since it is mostly located in hematopoietic cells and affects the lymphoid cell function unlike others.[18,19] In 2003, researchers at Pfizer reported tofacitinib as a JAK3 inhibitor,[20] however, later it was identified as a pan-JAK inhibitor.[21] The fact that it suppresses all JAK-STAT signal pathways explains its excellent potencies in many preclinical[22] and clinical trials.[23-25] Finally, tofacitinib became the first US Food and Drug Administration (FDA) approved oral drug for the treatment of rheumatoid arthritis in 2012 with a trade name Xeljanz.[26]

Using Pan-JAK inhibitors like tofacitinib for treatment is accompanied by some side effects since they inhibit all JAK isoenzymes. In particular, preclinical studies[27-29] and clinical trials[30,31] have revealed adverse effects derived from JAK2 inhibition like anemia, neutropenia, increased low and high density lipoprotein cholesterol levels, and elevated triglyceride levels. In the case of tofacitinib, similar adverse events have also been reported.[24,25,32] As a result, European Medicines Agency (EMA) refused the marketing authorization of tofacitinib in Europe.[33] Therefore the search for JAK1-selective inhibition has received considerable attention[34] since it has been revealed that JAK1 inhibition plays a pivotal role on the efficacies of tofacitinib.[35]

[a] *Department of Chemistry, College of Natural Sciences, Seoul National University, Seoul 08876, South Korea.*
[b] *Yang Ji Chemical Co., Ltd., Gyeonggi Bio-Center, Suwon, Gyeonggi-do 16229, South Korea.*
[c] *Han Wha Pharma Co., Ltd., 109, Yagam-gil, Nam-myeon, Chuncheon, Gangwon-do 24468, South Korea.*
† These two individuals contributed equally to this work.
Electronic Supplementary Information (ESI) available: Detailed experimental procedures of representative compounds and analytical characterisation of all compounds. See DOI: 10.1039/x0xx00000x

View Article Online
DOI: 10.1039/C7MD00568G

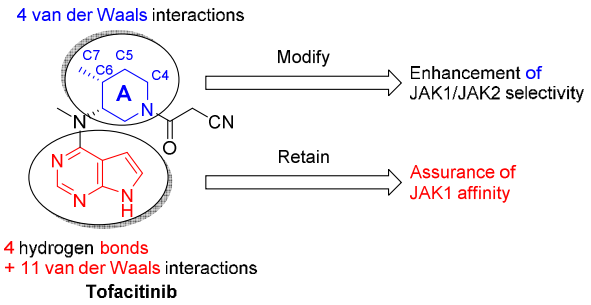

Figure 1 Design strategy by changing the piperidine moiety A.

Among various JAK1-selective inhibitors,[36] Galapagos' filgotinib[37,38] is known to be highly selective for JAK1 over JAK2 by 27.7 times. Its IC_{50}'s against IL-6/JAK1/pSTAT1 and GM-CSF/JAK2/pSTAT5 are 629 nM and 17,453 nM, respectively.[39] From collagen-induced arthritis (CIA) mouse and rat models, its efficacy was shown to be similar to etanercept, a TNF-α blocker.[40] Through the phase IIa proof-of-concept study, the hypothesis was proven that rheumatoid arthritis can be ameliorated by treatment with JAK1-selective inhibitors.[41] In 2016, Galapagos and Gilead went into phase III clinical studies.[42-44] Despite its advantages, the reported preclinical results indicated that it induced testicular toxicity in rats and dogs. Thus, the US FDA approved a lower male maximum clinical dosage than for the female one.[45] Therefore, new JAK1-selective drugs overcoming the toxicological weakness need to be developed. Another promising candidate compound in this class is upadacitinib in phase III by AbbVie.[46,47] Although not much toxicological information on the preclinical and clinical trials of upadacitinib is available, its IC_{50}'s for JAK1 and JAK2 in cellular assay were reported to be 8 nM and 600 nM, respectively, indicating 74-fold selectivity.[48]

We have initiated our investigation on new JAK1-selective inhibitors based on 5-azaspiro[2.4]heptan-7-amine core structure for subjugating the filgotinib limitation. New lead compounds were obtained, which met the criteria set by us for treating rheumatoid arthritis. Herein we describe the design, synthesis and improved pharmaceutical efficacies of our inhibitors.

Strategy

Since tofacitinib is known to interact with the binding sites of ATP as a competitive inhibitor for JAK isozymes, we focused our attention on the structure of tofacitinib, which resembles adenosine triphosphate (ATP) minus the triphosphate group.[49] According to the X-ray crystallography of tofacitinib at JAK1 or JAK2 reported by N. K. Williams *et al*.,[50] the most important interaction of tofacitinib in its binding with JAKs appears to come from the pyrrolopyrimidine ring: it interacts with JAK1 with 4 hydrogen bonds and 11 van der Waals interactions. The next important interactions are 4 van der Waals interactions with four carbon atoms (C4 – C7) at the piperidine ring. We envisioned that, to tune the inhibition selectivity for JAK1 over JAK2, new structural motifs could be explored for the substituted aminopiperidine moiety.

Synthesis

Scheme 1 Synthesis of inhibitors containing various heterocyclic core units replacing the aminopiperidine unit of tofacitinib and substituted *N*-methyl-*N*-(5-azaspiro[2.4]heptan-7-yl)-7H-pyrrolo[2,3-*d*]pyrimidin-4-amines.

View Article Online
DOI: 10.1039/C7MD00568G

Various monocyclic and bicyclic nitrogen containing compounds **6a – 6g** were synthesized for the selection of the most optimal scaffold at the position A in Figure 1 as shown in Scheme 1. Commercially available 4-amino-1-benzylpiperidine and (*R*)-3-amino-1-benzylpiperidine were converted to the *N*-ethyloxycarbonyl protected compounds, which were treated with LAH to result in the formation of methylamine derivatives **3a** and **3b**. The key pyrrolidine component of compound **6c**, 5-((*R*)-1-phenylethyl)-5-azaspiro[2.4]heptan-7-amine, was prepared according to the method reported by Y. Kimura and colleagues.[51] We obtained each diastereomer of 5-((*R*)-1-phenylethyl)-5-azaspiro-[2.4]heptan-7-amine with the carbon 7 as an epimeric center. Methylated compound **3c** was obtained through the above method from 5-((*R*)-1-phenylethyl)-5-azaspiro[2.4]heptan-7-amine. Compound **3d** was synthesized through debenzylation of **2c**. A bis(hydrochloric acid) salt form of bicyclic amine **3e**, (*R*,*R*)-6-benzyl-octahydro-pyrrolo[3,4-*b*]pyridine dihydrochloride, was purchased from Sigma-Aldrich, USA. Commercially available compounds such as 4-hydroxypiperidine and *rac*-3-hydroxymethylpiperidine were converted to the corresponding benzylated amines, **3f** and **3g**.

The obtained amines and alcohols, **3a – 3g**, were used for the coupling with 6-chloro-7-deazapurine in presence of K_2CO_3 in an aqueous solution, leading to compounds **4a – 4g**. We then performed debenzylation of **4a-c** and **4e-f** using palladium on carbon and ammonium formate to remove benzyl and (*R*)-1-phenylethyl protection groups, obtaining **5a-c** and **5e-f**. In the case of **5d**, *N*-ethyloxycarbonyl group of **4d** was deprotected with 1 N aqueous hydrochloric acid under reflux condition. From compounds **5a – 5g** the corresponding amide couplings were carried out with ethyl cyanoacetate in the presence of 1,8-diazabicyclo[5.4.0]undec-7-ene (DBU) at 80 °C as shown in Scheme 1, leading to compounds **6a – 6g**. Since the inhibitor **(*R*)-6c** synthesized from 7(*R*)-5-((*R*)-1-phenylethyl)-7-amino-5-azaspiro[2.4]heptane **(*R*)-1c** showed the most promising inhibition selectivity between JAK1 and JAK2, we focused our efforts on compound **(*R*)-6c**. Amine **(*R*)-4c** was transformed to the final compounds **7 – 56** through various reactions at the pyrrolidine nitrogen.

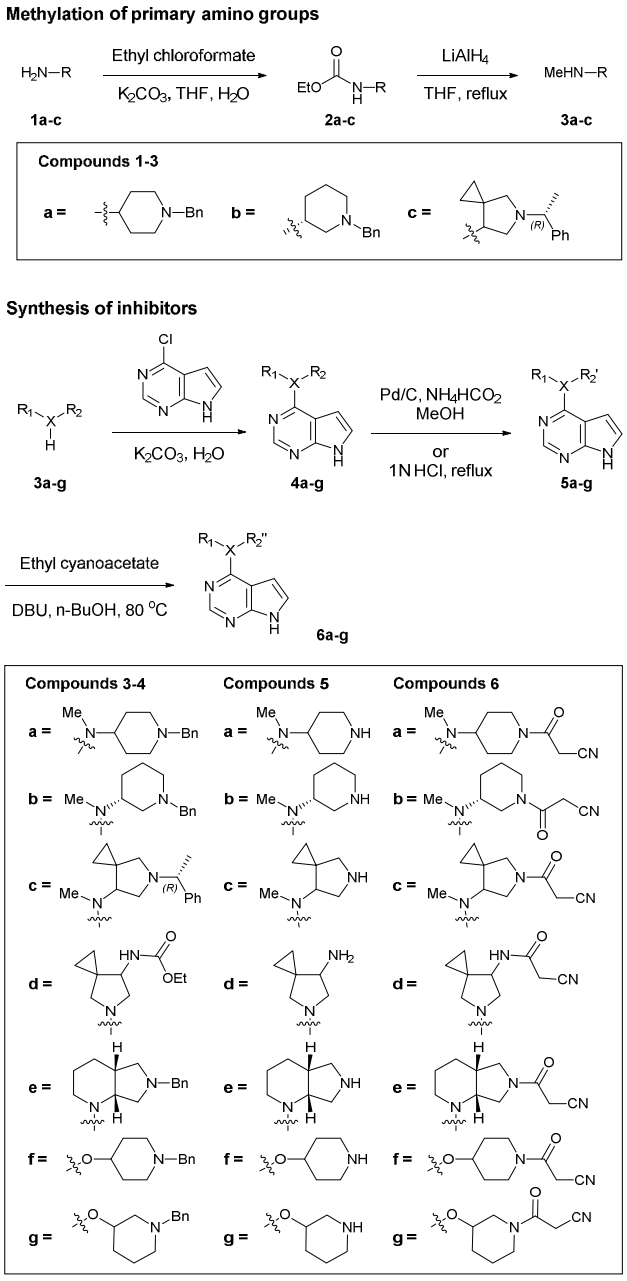

Results and discussions

Enzyme assay

For the selection of a new scaffold, we first screened substituted piperidine and pyrrolidine scaffolds at the position A in Figure 1 (Table 1). Each compound was evaluated for inhibition against JAK1 and JAK2 at 1 μM concentration. In the case of **6a** and **6f**, the inhibition abilities against JAK1 and JAK2 do not appear to be influenced by the connecting atom (nitrogen vs oxygen) at the C(4) position of piperidine. However, the amino-substitution position at the piperidine ring appeared to be an important factor for determining affinities for not only JAK1 but also JAK2. Between **6a** and **6b**, the substitution at the C(3) position of piperidine (**6b**) was more favoured for both JAK1 and JAK2 inhibitions than the substitution at the C(4) position (**6a**) was. The substitution with methyloxy group (**6g**) was disfavoured for JAK1 affinity. In the case of **6e**, introduction of the bicyclic (4a*R*,7a*R*)-octahydro-1H-pyrrolo[3,4-b]pyridine lowered the inhibition against JAK1. In introducing 5-azaspiro-[2.4]-heptan-7-amine moiety, the substitution position was important. While compound **6c** exhibited strong inhibition against JAK1, **6d** displayed very low inhibition against JAK1. Though both **6b** and **6c** showed strong inhibition against JAK1, **6b** showed high inhibition on JAK2 as well. Therefore, we

View Article Online
DOI: 10.1039/C7MD00568G

Table 1 Screening of the hydrophobic moieties (moiety A)

Compound	A	Inhibition% at 1 μM	
		JAK1	JAK2
6a	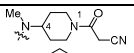	49%	1%
6b	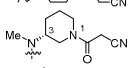	99%	83%
6c	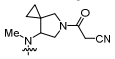	95%	53%
6d	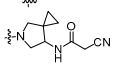	6%	10%
6e	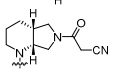	54%	-7%
6f	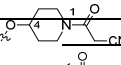	35%	5%
6g	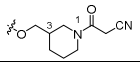	30%	10%

Table 2 Comparison of JAK1 IC_{50} values of 3-(7-(methyl(7*H*-pyrrolo[2,3-*d*]pyrimidin-4-yl)amino)-5-azaspiro[2.4]heptan-5-yl)-3-oxopropanenitrile racemate and enantiomers

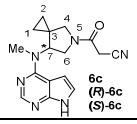

Compound	Configuration at 7-position	JAK1 IC_{50} (nM)
6c	racemate	29
(*R*)-6c	(*R*)	8.5
(*S*)-6c	(*S*)	790

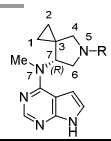

Cmpd	R	IC_{50} (nM)	SI[a]	Cmpd	R	IC_{50} (nM)	SI[a]

than those with short alkyl groups, but was disfavoured against JAK2 (120 nM in JAK1 vs 98000 nM in JAK2). The inhibitor with the benzylamine group displayed its selectivity index of 820 for JAK1 over JAK2.

As for inhibitors with amide groups at the pyrrolidine nitrogen, those with cyanoacetyl and azidoacetyl substitutions (**(*R*)-6c** and **10**, respectively) were quite potent against JAK1 with the IC_{50} values of 8.5 and 21 nM, respectively. A slightly larger isovaleric amide **11** exhibited comparable activity for JAK1 inhibition. It is interesting to note that two similarly-sized amides, isobutyramide **12** and cyclopropanecarboxamide **13**, selected **6c** as our scaffold for further SAR studies for finding inhibitors with high JAK1/JAK2 selectivity.

Our further SAR study was based upon **5c** as a scaffold for derivatives on the pyrrolidine nitrogen. When a racemic mixture **6c** was tested against the JAK1 isozyme (Table 2), it showed an IC_{50} value of 29 nM, proving that it could be used as a good lead for new JAK1 inhibitors. Then we investigated each enantiomer of **6c**. Compound **(*R*)-6c** exhibited 8.5 nM against JAK1, whereas 790 nM IC_{50} was observed with the enantiomeric **(*S*)-6c**. As a result, for further SAR studies the (*R*)-configuration of 7-amino-5-azaspiro[2.4]heptane was chosen.

In the cases of *N*(5)-alkylated compounds **7**, **8**, and **9**, inhibitor **9** having an *N*-benzyl group showed higher affinity to JAK1

Table 3 The IC_{50} values against JAK1 and JAK2 with the selectivity indices of substituted (*R*)-*N*-methyl-*N*-(5-azaspiro[2.4]heptan-7-yl)-7H-pyrrolo[2,3-*d*]pyrimidin-4-amines

View Article Online
DOI: 10.1039/C7MD00568G

		JAK1	JAK2				JAK1	JAK2	
7		1400	30000	21	**26**	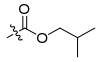	34	1200	35
8		230	15000	65	**27**	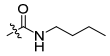	75	2800	37
9		120	98000	820	**28**	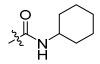	69	4400	64
(*R*)-6c		8.5	410	48	**29**	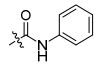	12	420	35
10		21	250	12	**30**	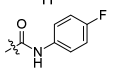	23	1000	43
11		77	1100	14	**31**	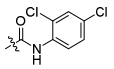	120	4700	39
12		170	2800	16	**32**	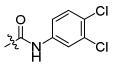	40	1300	33
13		170	1200	7.1	**33**	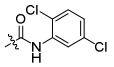	54	2800	52
14		520	16000	31	**34**	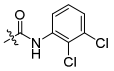	74	1300	18
15		670	13000	19	**35**	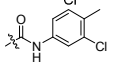	85	1300	15
16	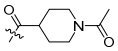	180	2500	14	**36**		1500	9100	6.1
17		53	930	18	**37**	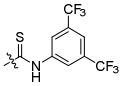	470	11000	23
18		150	6300	42	**38**		7.2	180	25
19		160	7800	49	**39**		20	130	6.5
20		140	6500	46	**40**		6.9	36	5.2
21	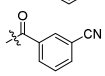	100	7400	74	**41**		9.0	51	5.7
22	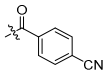	190	4500	24	**42**		13	97	7.5
23		500	9100	18	**43**		2.8	8.4	3.0
24	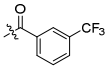	420	11000	26	**44**		9.4	50	5.3
25		20	160	8.0	**45**		50	480	9.6

[a] SI, Selectivity Index = JAK2 IC_{50} / JAK1 IC_{50}

Table 3 The IC_{50} values against JAK1 and JAK2 with the selectivity indices of substituted (*R*)-*N*-methyl-*N*-(5-azaspiro[2.4]heptan-7-yl)-7H-pyrrolo[2,3-*d*]pyrimidin-4-amines (continued)

Cmpd	R	IC_{50} (nM)	SI[a]	Cmpd	R	IC_{50} (nM)	SI[a]

View Article Online
DOI: 10.1039/C7MD00568G

		JAK1	JAK2				JAK1	JAK2	
46	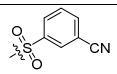	5.8	59	10	**52**	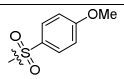	9.3	180	19
47	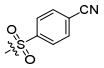	9.8	1100	110	**53**	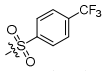	16	1400	88
48		26	470	18	**54**	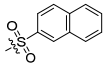	17	150	8.8
49	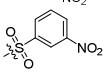	1.4	5.5	3.9	**55**		15	150	10
50	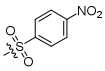	6.3	30	4.8	**56**		31	260	8.4
51	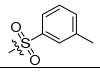	12	66	5.5					

[a] SI, Selectivity Index = JAK2 IC_{50} / JAK1 IC_{50}

exhibited similar JAK1 inhibitions. However, compound **12** showed a higher selectivity index against JAK2 than **13**. This tells us that there may be a more sensitive structural interaction in JAK2 with the amide motif. Amides substituted with a polar group like compounds **14** – **16** did not show significant inhibition against JAK1. Aroyl amides **18**– **24** also showed IC_{50} values in a 100-1000 nM range except for the small 2-furanoyl amide **17**, which gave 53 nM IC_{50} against JAK1. This indicates again that a large amide group at the pyrrolidine nitrogen is not tolerated well in the JAK1 binding site.

The transition from an amide to a thioamide lowered the inhibition activity against JAK1, but not so much against JAK2 that the inhibitor possessing 2-cyanoethanethioamide exhibited a lower selectivity index than that with 2-cyanoacetate (**(*R*)-6c** vs **25**). Introducing a urethane (**26**) into the pyrrolidine nitrogen resulted in considerable potency (IC_{50} = 34 nM) against JAK1 with a selectivity index of 35. Urea compounds (**27** – **36**), except for **31** and **36**, exhibited two-digit nanomolar IC_{50}'s against JAK1. For ureas made up with aliphatic amines, 1-butylurea **27** and 1-cyclohexylurea **28** showed similar affinities for JAK1 with IC_{50} values of 75 and 69 nM, respectively. However, compound **28** with a cyclic alkyl urea group was inferior in the JAK2 inhibition with IC_{50}'s of 4400 nM to the acyclic urea **27** with 2800 nM IC_{50}. Comparing 1-cyclohexyl urea **28** and phenyl urea **29** indicates that the inhibition abilities of the latter were higher in both JAK1 and JAK2 with IC_{50}'s of 12 nM and 420 nM, respectively. Halide-substituted phenyl ureas **30** – **35** did not show any improvements in inhibitory activities compared to the parent phenyl urea, **29**. When the phenyl group of the phenyl urea was substituted with an *ortho*-phenyl group (compound **36**), the inhibition of JAK1 and JAK2 decreased precipitously with IC_{50} values of 1500 and 9100 nM, respectively, presumably due to increased steric hindrance.

In the case of sulfonamides, most compounds displayed strong inhibition against the two enzymes. Some inhibitors showed single digit nanomolar range IC_{50}'s against JAK1. When amides and sulfonamides of similar sizes were compared, in all cases the inhibitors possessing a sulfonamide showed increased affinities for JAK1: the IC_{50}'s of **12** vs **39**, **18** vs **41**, **21** vs **46**, and **22** vs **47** were 170 vs 20, 150 vs 9.0, 100 vs 5.8, and 190 vs 9.8 nM, respectively. However, the sulfonamide inhibitors also increased their inhibition against JAK2, leading to lower selectivity indices than those of amide inhibitors. The JAK1 affinity appeared to be quite sensitive towards the substituent on benzenesulfonamide (**42** – **50**): the *meta*-substitution gave the best inhibition whereas the *ortho*-substitution showed the lowest affinities for the JAK1 isozyme.

According to our enzyme assays, **(*R*)-6c** and **46** seemed to be more selective for JAK1 over JAK2 than filgotinib, of which the IC_{50}'s are 10, 28, 810, and 116 nM for JAK1, JAK2, JAK3, and TYK2, respectively.[40] Therefore, we selected two representative compounds, **(*R*)-6c** and **46** for additional evaluation against JAK3 and TYK2. The IC_{50} of **(*R*)-6c** on JAK3 and TYK2 were 1100 and 250 nM with the selectivity indices of 130 and 29, respectively. For **46**, 110 and 25 nM IC_{50}'s were observed for JAK3 and TYK2, respectively.

Docking simulation

View Article Online
DOI: 10.1039/C7MD00568G

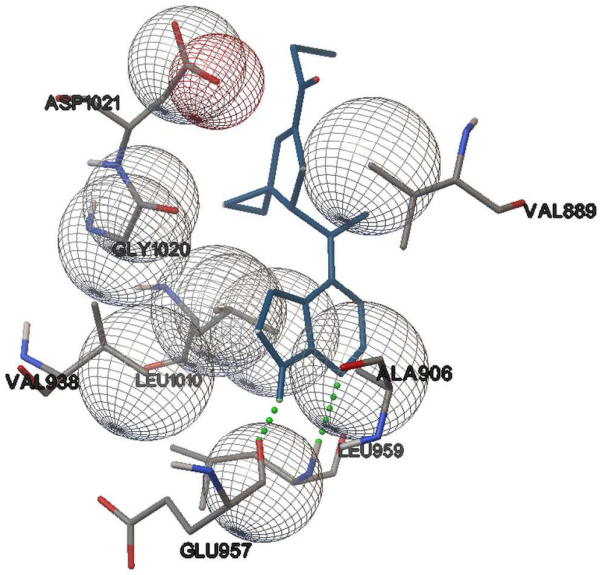

Figure 2 Flexible docking simulation of **(*R*)-6c** with JAK1 (PDB ID: 3EYG) by AutoDock 4.2.[51]

To probe the validity of our approach with a molecular modelling, we examined a flexible docking simulation of our representative compound **(*R*)-6c** with JAK1 (PDB ID: 3EYG) by AutoDock 4.2[52] (Figure 2). It appeared that its pyrrolopyrimidine moiety can bind to Ala906, Glu957 and Leu959 of JAK1 through hydrogen bonds and van der Waals interactions. Moreover, the (*R*)-5-azaspiro[2.4]heptan-7-amine moiety of **(*R*)-6c** was expected to interact with Val889 and Gly1020. As a result, the above strategy of modifying the aminopiperidine moiety seems to be suitable in finding a new JAK1-selective inhibitor.

In vitro ADME studies on (*R*)-6c, 38, and 46

Several *in vitro* ADME profiles such as plasma stability, protein binding, liver microsomal stability, Caco-2 permeability, and cytochrome P_{450} inhibition for selected JAK1 inhibitors, **(*R*)-6c**, **38** and **46**, were investigated. First, over 98% of **38** and **46** remained in human and rat plasma for 120 minutes (Table 4). In the case of **(*R*)-6c**, 98.5% remained in human plasma for the same duration, showing similar stabilities as **38** and **46**. However, in rat plasma, 89.6% of **(*R*)-6c** remained after 120 minutes. Therefore, it can be concluded that most tested compounds remained as their parent drug structures in plasma. In human plasma protein binding tests (Table 5), the bound proportion of **(*R*)-6c** was 29.8%, which was similar to that of tofacitinib citrate and filgotinib, 39% and 31.8%, respectively.[33,39] However, **38** and **46**, both of which have sulfonamide groups, showed higher protein binding – 44.4% and 87.4%, respectively. The results correlate well with their lipophilicities: the LogP values of their neutral forms gradually increase in the order of amide **(*R*)-6c**, aliphatic sulfonamide **38**, and aromatic sulfonamide **46**.

To probe the stability of the selected compounds in the liver first-pass, liver microsomal stabilities were examined (Table 6). The remaining compound **(*R*)-6c** (94.6%) after 30-minute incubation in human liver microsomes was similar to that of filgotinib (87% after 60-minute incubation).[39] While compound **38** possessing an ethanesulfonamide group was less stable than filgotinib, with 79.7% remaining after 30 minutes, the *m*-cyanophenylsulfonamide-containing compound **46** was heavily metabolized in human liver microsomes and only 6.0% remained after 30 min incubation.

Table 4 Plasma stabilities of **(*R*)-6c**, **38**, and **46**

Compound	Human (% remaining)		Rat (% remaining)	
	30 min	120 min	30 min	120 min
(*R*)-6c	95.0	98.5	98.4	89.6
38	> 100	> 100	> 100	> 100
46	96.6	98.6	> 100	> 100

Table 5 Plasma protein binding and LogP values of **(*R*)-6c**, **38**, and **46**

Compound	Human (% bound)	Rat (% bound)	LogP (neutral X)
(*R*)-6c	29.8	18.7	1.69
38	44.4	49.5	2.07
46	87.4	85.8	3.69

Table 6 Liver microsomal stabilities of **(*R*)-6c**, **38**, and **46**

Compound	% Remaining after 30 min			
	Human (%)	Dog (%)	Rat (%)	Mouse (%)
(*R*)-6c	94.6	99.9	84.8	84.9
38	79.7	56.1	22.9	33.9
46	6.0	5.5	2.4	3.2

Table 7 Caco-2 permeabilities of **(*R*)-6c**, **38**, and **46**

Compound	P_{app}, A to B (10^{-5} cm/sec)	P_{app}, B to A (10^{-5} cm/sec)	Efflux ratio
(*R*)-6c	0.66	1.85	2.78
38	2.54	2.56	1.01
46	1.34	1.57	1.17

To probe drug-drug interaction possibilities, we screened compounds **(*R*)-6c**, **38**, and **46** against representative CYP_{450} isoforms at 10 μM concentrations for each compound (Table 8). CYP 2C19 and 2E1 were influenced at the same concentrations of **(*R*)-6c**. Compound **38** seemed to inhibit only CYP 2E1 isoform at the concentration. However, **46** treatment was likely to affect many isoforms including CYP 1A2, 2C8, 2C9, 2C19, 2E1, and 3A4, which may lead to possible interactions with many drugs. The CYP 2E1 isoform, which **(R)-6c**, **38**, and **46** commonly inhibited, has substrates for some anaesthetics like halothane, enflurane, methoxyflurane, sevoflurane, and so on.[53] Representative substrates of CYP 2C19 comprise proton pump inhibitors including esomeprazole, lansoprazole, and so on. In the case of the proton pump inhibitors, their prescription frequencies are decreasing in recent times, so that the combined prescription would not be a problem.

Due to high plasma protein binding, low liver microsomal stability, and high CYP_{450} inhibition rates, we excluded

View Article Online
DOI: 10.1039/C7MD00568G

Table 8 The inhibition percentages against CYP_{450} isoforms of **(*R*)-6c**, **38**, and **46**

Compound	CYP_{450} isoforms (% of control activity @ 10 μM)								
	1A2	2A6	2B6	2C8	2C9	2C19	2D6	2E1	3A4
(*R*)-6c	92.5	92.0	91.5	81.0	84.4	66.0	91.6	50.3	89.7
38	99.9	96.7	> 100	> 100	90.7	93.8	> 100	63.9	95.4
46	65.7	87.2	92.0	66.2	50.4	55.8	90.3	59.8	33.2

compounds with sulfonamide groups from further studies. Therefore, **(*R*)-6c** was chosen for studies on hERG, kinase profiling, and *in vivo* efficacy tests.

Table 9 Pharmacokinetic parameters of the free base and the salt forms of **(*R*)-6c** in Sprague-Dawley rats

Sample	**(*R*)-6c**							
Salt form	Free base		Hydrochloride		Citrate		Tartrate	
Route	P.O.	I.V.	P.O.	I.V.	P.O.	I.V.	P.O.	I.V.
N (S.D. Rat)	4M	4M	4M	4M	4M	4M	4M	4M
Dose (mg/kg)	10	5	10	5	10	5	10	5
C_{max} (ng/mL)	1000		1300		1200		1000	
T_{max} (h)	0.30		0.40		0.50		0.40	
$t_{1/2}$ (h)	2.1	1.2	1.1	0.60	3.6	4.3	1.0	1.0
$AUC_{0\rightarrow inf}$ (ng·h/mL)	2100	920	2400	1900	2400	2000	1900	1400
$AUC_{0\rightarrow t}$ (ng·h/mL)	1900	900	2400	1800	2400	2000	1900	1400
MRT (h)	3.1	1.1	1.6	0.7	2.3	1.2	1.5	0.9
F (%)	110		65		58		68	

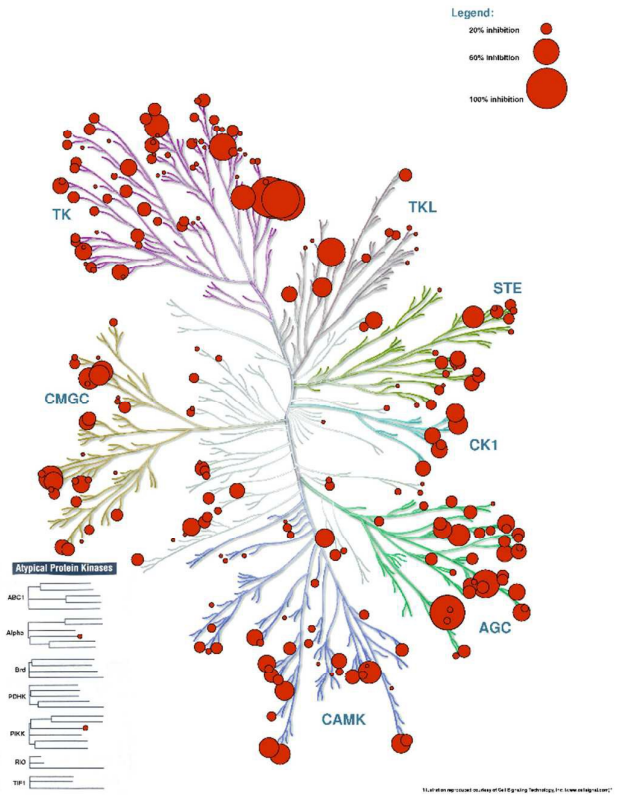

Figure 3 The kinome tree of **(*R*)-6c** against 323 kinases at the 10 μM concentration drawn by the web accessible Kinome Render program.[57]

Human ether-a-go-go related gene (hERG) potassium channel assays and kinase profiling

Next, we investigated the hERG binding of **(*R*)-6c** for its cardiotoxicity prediction. The binding test was carried out with HEK293 cells according to the automated patch clamp method with IC_{50} of $1.2x10^2$ μM. Under the same conditions, filgotinib gave IC_{50} of 85 μM. From these results, **(*R*)-6c** appears to be superior to filgotinib in the cardiotoxicity at the same blood concentration predicted by the hERG assay.

View Article Online
DOI: 10.1039/C7MD00568G

Ki… a
pr… ne
ta… de
ef… at
th… ıly
fo… <2
sh… %
inl…

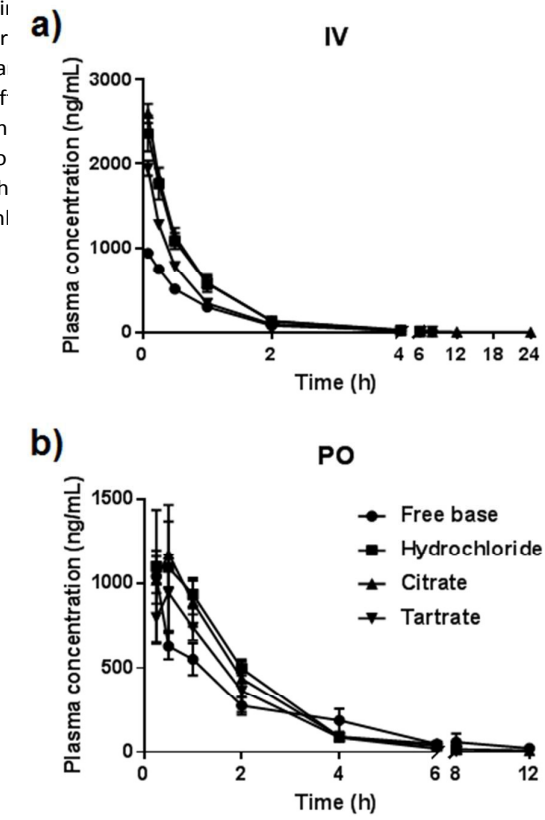

Figure 4 Plasma concentrations after a) intravenous injection and b) oral administration of the free base and the salt forms of **(*R*)-6c** in Sprague-Dawley

Rodent pharmacokinetics of (*R*)-6c

To determine the dosage for *in vivo* efficacy tests, we investigated the pharmacokinetic profiles of **(*R*)-6c** in rats (Table 9). In the case of the oral administration at the 10 mg/kg dose, the pharmacokinetic profiles of **(*R*)-6c** were obtained as follows: the maximum concentration (C_{max}) of 1000 ng/mL, the time to reach the maximum concentration (T_{max}) of 0.30 hour, the half-life ($t_{1/2}$) of 2.1 hours, and the area under the curve from time 0 to infinite time ($AUC_{0\rightarrow inf}$) of 2100 ng·h/mL. However, the bioavailability of **(*R*)-6c** exceeded 100%. This is presumed to be caused by the use of PEG400 as a vehicle to overcome poor water solubility, which apparently lowered the compound's i.v. exposure.[54] To improve **(*R*)-6c** exposure in the *in vivo* model, we made several different salts using hydrochloride, citric acid, and tartaric acid (Figure 4). For hydrochloride and citrate salts, their drug exposures were increased by 26% compared to the free base form. However, the tartrate salt was relevantly less exposed than the free base in the oral administration. Moreover, the citrate form had the additive advantage that its half-life was elongated to 3.6 hours. Hence, the citrate form appears to be the preferred formulation in oral administration.

In vivo efficacy studies on (*R*)-6c

Both collagen-induced arthritis (CIA) and adjuvant-induced arthritis (AIA) are well-established animal models for the testing and development of new RA therapeutics.[55,56] We used these models to evaluate the efficacies for the treatment with

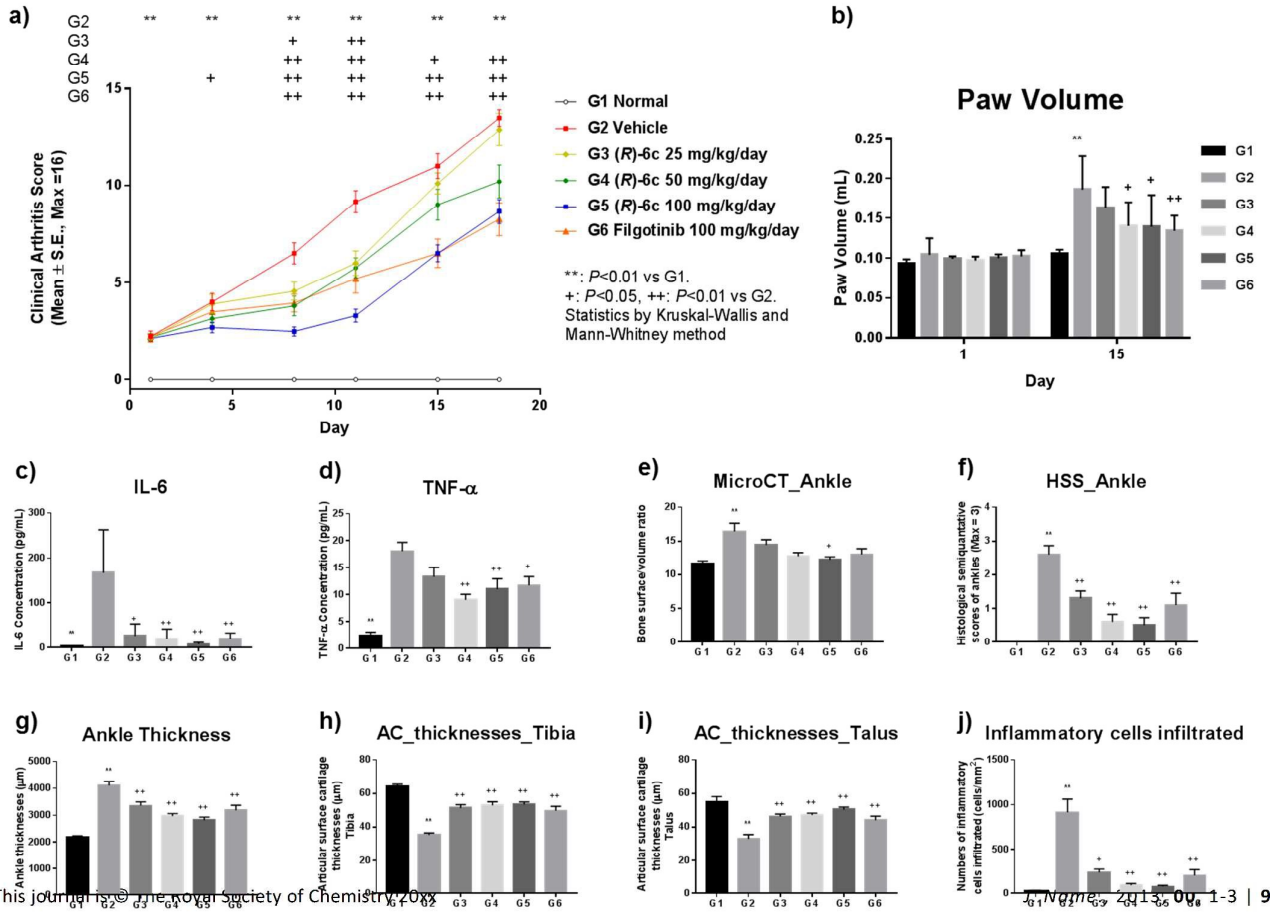

Figure 5 Effects of **(*R*)-6c** treatment on collagen-induced arthritis in DBA/1J mice: a) the clinical arthritis scores for 18 days, b) the volumes of right hind paws on days 1 and 15, c-d) the concentrations of IL-6 and TNF-α, respectively, at the serums sampled after autopsy, e) the bone surface/volume ratios of right hind ankle joints measured by micro-CT, f) the histopathological semiquantitative scores of right hind ankle joints, g) the right hind ankle joint thicknesses, h-i) the articular surface cartilage thicknesses (tibia and talus) in right hind ankle joints, and j) the numbers of inflammatory cells infiltrated in the right hind ankle joints. The significance symbols are ** = significantly different between G1 and G2 (P <0.01), + = significantly different from G2 (P <0.05), and ++ = significantly different from G2 (P <0.01)

View Article Online
DOI: 10.1039/C7MD00568G

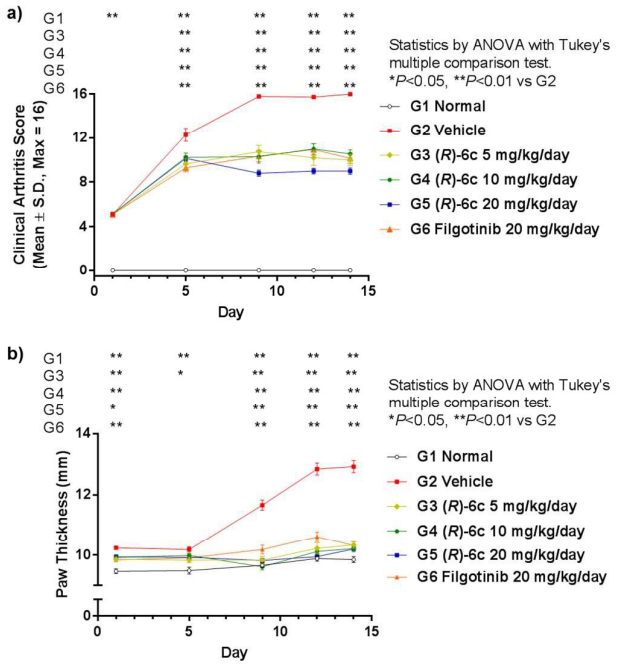

Figure 6 Effects of **(*R*)-6c** treatment on adjuvant-induced arthritis in Lewis rats: a) the clinical arthritis scores and b) the volumes of right hind paws. The data were measured twice per week for 14 days.

(*R*)-6c in a free base form. In the mouse CIA study, the effect of **(*R*)-6c** treatment was evaluated by using the following indices: clinical arthritis score, paw volume, serum cytokine concentration, bone surface/volume ratio, and histopathological data of ankles. Filgotinib (100 mg/kg/day)[40] was used as a positive control. Treatment with **(*R*)-6c** (25, 50 or 100 mg/kg/day) resulted in significant attenuation of arthritis in DBA1/J mice when compared to vehicle treatment (Figure 5). Compound **(*R*)-6c** treatment ameliorated clinical arthritis score, paw volume, serum IL-6 concentration, bone surface/volume ratio and histopathological parameters in a dose-dependent manner. Furthermore, at the doses of 50 and 100 mg/kg/day, **(*R*)-6c** treatment exhibited more favourable results than filgotinib treatment did in clinical arthritis score, cytokine levels, bone surface/volume ratio and all histopathological features.

In the rat AIA study (Figure 6), all treatments with test articles significantly suppressed the arthritis symptoms versus vehicle treatment for 14 days. The treatment with 20 mg/kg/day of **(*R*)-6c** demonstrated higher efficacy than that of filgotinib (20 mg/kg/day). The clinical arthritis scores at the dosage of 5, 10, and 20 mg/kg/day of **(*R*)-6c** reached 10.0, 10.6, and 9.0 values, respectively, and paw thicknesses were 10.33, 10.21, and 10.20 mm, respectively, at day 14. However, filgotinib showed slightly inferior clinical arthritis score (10.2) and paw thickness (10.32 mm) (day 14) compared to **(*R*)-6c** at the same dosage.

Experimental sections

Chemistry

The synthetic methods of representative compounds and the spectroscopic data of all compounds are described in Electronic Supplementary Information (ESI).

In vitro enzyme assays and kinase profiling

All enzyme inhibition assays including kinase profiling results were obtained from commercially available kinase binding activity assay, KinaseProfiler™ services (Eurofins Scientific, UK).[57] All kinase binding activity assays were performed at K_m values for ATP. The 50% inhibitory concentration (IC_{50}) of each compound was determined with GraphPad Prism software. The kinome tree of the inhibition percentages of 323 kinases at the 10 μM concentration for **(*R*)-6c** was drawn by R. Najmanovich's Kinome Render web accessible tool.[58]

In vitro ADME assays

All *in vitro* ADME, including plasma stability, plasma protein binding, liver microsomal stability, Caco-2 permeability, and hERG assays, were performed by commercially available services at the New Drug Development Center, Daegu-Gyeongbuk Medical Innovation Foundation, South Korea and Drug Discovery Platform Technology Group, Korea Research Institute of Chemical Technology, South Korea. Plasma stability, plasma protein binding, liver microsomal stability, Caco-2 permeability, and CYP_{450} inhibition tests were analysed by LC-MS/MS, Nexera XR system (Shimadzu, Japan) with TSQ vantage triple quadruple (Thermo, USA). The column was Kinetex XB-C18 column (2.1x100 mm, 2.6 μm particle size; Phenomenex, USA) and the obtained data were analysed in Xcalibur program (version 1.6.1).

Plasma stability assay

Human or rat plasma was treated with test articles at 10 μM concentration. Procaine and diltiazem were used for positive controls. The plasma tubes were incubated at 37 °C for 0, 30, and 120 minutes. Acetonitrile including internal standard, chlorpropamide, was added to the tube, which was vortexed and centrifuged with a power of 14,000 rpm at 4 °C. After the centrifugation, the supernatant was analysed by LC-MS/MS.

Plasma protein binding test

Rapid equilibrium dialysis (RED) method was used for plasma protein binding test. Positive controls were dexamethasone and warfarin. Human or rat plasma was treated with test articles at 10 μM concentration. The same volumes of the treated plasma and phosphate-buffered saline (PBS, pH 7.4) were placed in RED chamber. The chamber was incubated at 37 °C for 4 hours. The same volumes of the incubated plasma and buffer were sampled and the same volumes of buffer and blank plasma were added, respectively. Acetonitrile including internal standard, chlorpropamide, was added to each sample tube, which was vortexed and centrifuged with a power of 14,000 rpm at 4 °C. After the centrifugation, the supernatant was analysed by LC-MS/MS.

Liver microsomal stability test

View Article Online
DOI: 10.1039/C7MD00568G

The liver microsome of human, dog, rat, or mouse (0.5 mg/mL), 0.1 M phosphate buffer, and a test article at 1 μM concentration were placed in a tube. Positive control was verapamil. The tube was incubated at 37 °C for 5 minutes. NADPH regeneration system solution was added to the tube, which were incubated at 37 °C for 30 minutes. Acetonitrile including internal standard, chlorpropamide, was added to the tube, which was vortexed and centrifuged with a power of 14,000 rpm at 4 °C. After the centrifugation, the supernatant was analysed by LC-MS/MS.

Caco-2 permeability assay

In a 12-well transwell, $1x10^6$ cells of Caco-2 cells (ATCC® HTB-37™) were seeded and they were grown for 3 weeks. Test article was diluted to 25 μM concentration with transport buffer (10 mM glucose, 4 mM sodium bicarbonate, and 1 mM 4-(2-hydroxyethyl)-1-piperazineethanesulfonic acid in Hank's balanced salt solution, pH 7.4). Positive controls were caffeine, ofloxacin, and atenolol. Of apical and basolateral chamber, test article was added to one chamber and then transport buffer was added to the other. During 60-minute incubation at 37 °C, samples from each chamber were taken every 15 minutes. The samples were diluted to 5 μM concentration with acetonitrile including internal standard, chlorpropamide. The samples were analysed by LC-MS/MS.

CYP inhibition test

A mixture of human liver microsomes (0.25 mg/mL), 0.1 M phosphate buffer, each cocktail including substrates for CYP_{450} isozymes, and test article at 0 or 10 μM concentration was incubated at 37 °C for 5 minutes. The cocktails are as follows: Cocktail A, phenacentin 50 μM + coumarin 2.5 μM + *S*-mephenytoin 100 μM + dextromethorphan 5 μM + midazolam 2.5 μM; Cocktail B, bupropion 50 μM + aminodaquine 2.5 μM + tolbutamide 100 μM + chlorzoxazone 50 μM. Then NADPH generation system solution was added and it was incubated at 37 °C for 15 minutes again. After the incubation, the reaction was quenched with acetonitrile including chlorphopamide as an internal standard. It was centrifuged with a power of 14,000 rpm at 4 °C. After the centrifugation, the supernatant was analysed by LC-MS/MS.

Human ether-a-go-go related gene (hERG) potassium channel assay

hERG assay was performed with automated planar patch clamp method in PatchXpress® 7000A (Molecular Devices, LLC., USA). HERG – HEK293 cells ($2 – 4x10^6$ cells) were placed in a 384 well-plate. Amphotericin B solution was added for perforated patch clamp and then it was placed for 10 minutes. To measure hERG normal current, The HEK293 cell membrane was held at -80 mV, and the current of potassium channel was measured while voltage was changed as follows: -40 mV for 100 milliseconds (ms), +40 mV for 500 ms, and -50 mV for 2 seconds. After measuring normal current with the mentioned method, the HEK293 cells were treated with test article solution at desired concentration. After 5 minutes, the current of potassium channel treated with test article was measured with the aforementioned method.

Pharmacokinetic study

Pharmacokinetic studies were performed with Sprague Dawley rats that were 7 to 8 weeks old. All groups consisted of four male rats fed freely for intravenous tests, but had fasted for 16 hours beforehand per oral tests. The dosages for intravenous and per oral tests were 5 and 10 mg/kg, respectively. The free base form of **(*R*)-6c** clearly dissolved under the vehicle condition of 10% ethanol and 90% PEG400 so the dose volume of 1 mL/kg is for intravenous administration. For oral administration, a suspension in corn oil was used, which has the 5 mL/kg dose volume. The salt forms include hydrochloride, citrate, and tartrate, which dissolved clearly in 100% saline so that their dose volumes became 250 and 2500 μL/kg for IV and PO, respectively. After their administrations, the blood samplings were performed at 0.08, 0.25, 0.5, 1, 2, 4, 6, 8, 12, and 24 hours for IV and at 0.25, 0.5, 1, 2, 4, 6, 8, 12, and 24 hours for PO. 20 μL of the sampled plasma was diluted with 180 μL of acetonitrile containing an internal standard. It was then vortexed and centrifuged under 15000 rpm at 4 °C. After the centrifugation, the supernatant was analyzed by LC-MS/MS, Nexera XR system (Shimadzu, Japan) with TSQ vantage triple quadruple (Thermo, USA). The column was Kinetex XB-C18 column (2.1 x 100 mm, 2.6 μm particle size; Phenomenex, USA) and pharmacokinetic parameters were obtained by the non-compartmental analysis model in Phoenix WinNonlin 6.4 version (Pharsight, USA). The animal care and procedure of this study were approved by the Animal Research Care Committee of New Drug Development Center, Daegu-Gyeongbuk Medical Innovation Foundation. The committee assures that the welfare of the animals was maintained in accordance with the requirements of the Animal Welfare Act of the Republic of Korea.

Mouse collagen-induced arthritis

Male DBA1/J mice (6 weeks old) were purchased from Japan SLC, Inc and all mice were housed in specific pathogen-free (SPF) conditions with free access to food and water. After 7 days of acclimation, mice were immunized with 0.1 mL of emulsion of 1:1 mixture of type II collagen (2 mg/mL) and complete Freund's adjuvant by subcutaneous injection at 1.5 cm distal from the tail base. After 21 days, immunized mice were boosted by another injection with 0.1 mL of emulsion of type II collagen and incomplete Freund's adjuvant. The emulsions were prepared according to manufacturer's instruction.[59] When all mice indicated signs of arthritis, treatment with test articles and assessment of arthritis were initiated (day 1). The immunized and boosted mice were randomized into 6 treatment groups (n=10 each) and same-aged naïve mice were assigned to a normal group (n=5). All test articles or vehicle were orally administered once daily and the clinical arthritis scores were assessed twice weekly for 18 days. Corn oil was used as a vehicle and all test articles were suspended in vehicle. The test article doses were 25, 50, and 100 mg/kg/day for **(*R*)-6c**, and 100 mg/kg/day for filgotinib.

View Article Online
DOI: 10.1039/C7MD00568G

Paw volumes were measured by LE7500 plethysmometer (Panlab, Spain) on days 1 and 15. The severity of each paw was evaluated and scored according to the following criteria where 0 = normal; 0.5 = redness of the toe, but not swollen; 1 = one toe inflamed and swollen; 2 = more than one toe, but entire paw, inflamed and swollen, or mild swelling of entire paw; 3 = entire paw inflamed and swollen; and 4 = very inflamed and swollen paw or ankylosed paw.[60] The clinical arthritis score was represented by the total scores of each paw. On day 19, all individuals were sacrificed and autopsies were performed. Serum cytokines including IL-6 and TNF-α were measured by ELISA kits (ProcartaPlex Mix and Match customized, Mouse 5 plex, BMS). For the histopathological studies, the right hind paws of each mouse were fixed by 10% formalin solution and the hematoxylin-eosin staining was performed on the ankle and third digit of the paw. The histopathological score was semiquantitatively measured according to the following criteria where 0 = normal; 1 = infiltration of inflammatory cells; 2 = synovial hyperplasia and pannus formation; and 3 = bone erosion and destruction.[61] The obtained images were analyzed by iSolution EL ver 9.1 (IMT i-solution Inc., Canada) and the micro-CT analyses of all individuals were performed by viviCT 80 micro-CT (SCANCO Medical, Switzerland) to measure bone surface/volume ratio. Student's *t*-test or one-way analysis of variance test was performed to determine statistically significant differences. The data for clinical arthritis scores were statistically analyzed by the Kruskal-Wallis test or Mann-Whitney test where a significant difference was defined as $P < 0.05$. The experimental protocol of the mouse study was approved by the Animal Research Care Committee of Gyeonggi Biocenter (Approval No. 2015-11-0019). The committee assures that the welfare of the animals was maintained in accordance with the requirements of the Animal Welfare Act of the Republic of Korea.

Rat adjuvant-induced arthritis

AIA was induced in SPF Lewis LEW/SsNSlc rats (Japan SLC Inc., Japan). After 2 weeks of acclimation, 10 week old rats were immunized by the subcutaneous injection of 0.1 mL of complete Freund's adjuvant containing 10 mg/mL of heat-killed mycobacterium (Chondrex, Inc., USA) at a 2.0 cm distal from the rat tail base. After 12 days of immunization (day 1), the rats were randomized into 6 treatment groups (n=10 each) and received test articles or vehicles alone once daily for 14 days. Same-aged naïve mice were assigned to a normal group (n=5). Corn oil was used as a vehicle and test article doses were 5, 10, and 20 mg/kg/day for **(*R*)-6c**, and 20 mg/kg/day for filgotinib. The clinical arthritis score and paw thicknesses were evaluated twice weekly for 14 days. The criteria for the clinical arthritis score are 0 = normal; 1 = mild edema or erythema; 2 = moderate edema; 3 = severe edema; and 4 = ankylosis. The paw thicknesses were measured by electric caliper CD-15CPX (Mitutoyo Corp., Japan). Kruskal-Wallis test or one-way analysis of variance test was performed to determine statistically significant differences, which were defined as $P < 0.05$. The experimental protocol of the rat study was approved by the Animal Research Care Committee of Qu-BEST BIO, Co., Ltd. (Approval No. QBSIACUC-A17001). The committee assures that the welfare of the animals was maintained in accordance with the requirements of the Animal Welfare Act of the Republic of Korea.

Conclusions

From the SAR studies hinged on the heterocyclic ring portion of the JAK1 inhibitors, we chose **(*R*)-6c** as our candidate for further evaluation and have shown the efficacy of **(*R*)-6c** through *in vitro* and *in vivo* tests. In the enzyme assays, the JAK1 IC_{50} value was 8.5 nM and the selectivity indices of JAK2 over JAK1 were 48.5, which were higher than those of filgotinib. In the kinase profiling, the inhibitory activities on other kinases were lower than on JAK series. From the above *in vitro* tests, we obtained highly JAK1-selective profiles for our inhibitor, which presumably would lead to lower toxicity.

In the *in vitro* ADME tests, its profiles were similar to those of filgotinib. The compound **(*R*)-6c** showed good human plasma stability along with two positive controls to exhibit similar profiles on the bound percentages on human plasma protein and the stability against human liver microsomes. Thus, there was a moderate permeability coefficient from A to B in Caco-2 permeability tests like filgotinib, but less efflux ratio so that it seems to be more highly permeable to cells than filgotinib. In the CYP_{450} isozyme screening, the compound showed inhibition of 2C19 and 2E1 isoforms at 10 μM concentrations. In pharmacokinetic studies in rats through oral administration, the profiles of the free base were at acceptable levels.

In the *in vivo* studies, **(*R*)-6c** relieved the arthritis symptoms more than an equivalent dose of filgotinib, the JAK1-selective inhibitor belonging to the same category, did. Taken together, our present study indicates that **(*R*)-6c** has desirable physicochemical properties and efficacy via selective inhibition of the JAK1 pathway. These findings suggest that **(*R*)-6c** has therapeutic potential for the treatment of rheumatoid arthritis.

Conflicts of interest

The authors declare no competing interests..

Acknowledgements

This research was performed with the DGMIF Drug Development Center and supported by the Bio & Medical Technology Development Program through the National Research Foundation of Korea (NRF); funded by the Ministry of Science, ICT & Future Planning (2014M3A9D9033717).

Notes and references

1 J. G. Stoll and U. Yasothan, *Nat. Rev. Drug Discov.*, 2009, **8**, 693.
2 C. Mount and J. Featherstone, J. *Nat. Rev. Drug Discov.*, 2005, **4**, 11.

View Article Online
DOI: 10.1039/C7MD00568G

3 K. D. Deane and H. El-Gabalawy, *Nat. Rev. Rheumatol.*, 2014, **10**, 212.
4 P. Jacques and F. Van den Bosch, *Expert Opin. Emerg. Drugs*, 2013, **18**, 231.
5 P. Emery, *Nat. Rev. Rheumatol.*, 2015, **11**, 69.
6 F. M. P. Meier, M. Frerix, W. Hermann and U. Müller-Ladner, *Immunotherapy*, 2013, **5**, 955.
7 G. R. Burmester, E. Feist and T. Dorner, *Nat. Rev. Rheumatol.*, 2014, **10**, 77.
8 E. Neumann, K. Khawaja and U. Muller-Ladner, *Nat. Rev. Rheumatol.*, 2014, **10**, 429.
9 S. Müller and S. Knapp, *Expert Opin. Drug Discov.*, 2010, **5**, 867.
10 V. Kelly and M. Genovese, *Rheumatology*, 2013, **52**, 1155.
11 J. K. Buer, *Inflammopharmacology*, 2015, **23**, 163.
12 T. Doan and E. Massarotti, *J. Clin. Pharmacol.*, 2005, **45**, 751.
13 J. R. O'Dell, *N. Engl. J. Med.*, 2004, **350**, 2591.
14 J. Detert and P. Klaus, *Biologics*, 2015, **9**, 35.
15 A. Mócsai, L. Kovács and P. Gergely, *BMC Med.*, 2014, **12**, 43.
16 A. F. Wilks, *Proc. Natl. Acad. Sci. U. S. A.*, 1989, **86**, 1603.
17 J. Darnell, I. Kerr and G. Stark, *Science*, 1994, **264**, 1415.
18 K. Shuai and B. Liu, *Nat. Rev. Immunol.*, 2003, **3**, 900.
19 K. Ghoreschi, A. Laurence and J. J. O'Shea, *Immunol. Rev.*, 2009, **228**, 273.
20 P. S. Changelian, M. E. Flanagan, D. J. Ball, C. R. Kent, K. S. Magnuson, W. H. Martin, B. J. Rizzuti, P. S. Sawyer, B. D. Perry, W. H. Brissette, S. P. McCurdy, E. M. Kudlacz, M. J. Conklyn, E. A. Elliott, E. R. Koslov, M. B. Fisher, T. J. Strelevitz, K. Yoon, D. A. Whipple, J. Sun, M. J. Munchhof, J. L. Doty, J. M. Casavant, T. A. Blumenkopf, M. Hines, M. F. Brown, B. M. Lillie, C. Subramanyam, C. Shang-Poa, A. J. Milici, G. E. Beckius, J. D. Moyer, C. Su, T. G. Woodworth, A. S. Gaweco, C. R. Beals, B. H. Littman, D. A. Fisher, J. F. Smith, P. Zagouras, H. A. Magna, M. J. Saltarelli, K. S. Johnson, L. F. Nelms, S. G. Des Etages, L. S. Hayes, T. T. Kawabata, D. Finco-Kent, D. L. Baker, M. Larson, M.-S. Si, R. Paniagua, J. Higgins, B. Holm, B. Reitz, Y.-J. Zhou, R. E. Morris, J. J. O'Shea and D. C. Borie, *Science*, 2003, **302**, 875.
21 D. M. Meyer, M. I. Jesson, X. Li, M. M. Elrick, C. L. Funckes-Shippy, J. D. Warner, C. J. Gross, M. E. Dowty, S. K. Ramaiah, J. L. Hirsch, M. J. Saabye, J. L. Barks, N. Kishore and D. L. Morris, *J. Inflamm*., 2010, **7**, 41.
22 M. E. Dowty, M. I. Jesson, S. Ghosh, J. Lee, D. M. Meyer, S. Krishnaswami and N. Kishore, *J. Pharmacol. Exp. Ther.*, 2014, **348**, 165.
23 E. Feist and G. R. Burmester, *Rheumatology*, 2013, **52**, 1352.
24 B. Bannwarth, M. Kostine and N. Poursac, *Expert Opin. Drug Metab. Toxicol.*, 2013, **9**, 753.
25 J. M. Kremer, B. J. Bloom, F. C. Breedveld, J. H. Coombs, M. P. Fletcher, D. Gruben, S. Krishnaswami, R. Burgos-Vargas, B. Wilkinson, C. A. F. Zerbini and S. H. Zwillich, *Arthritis Rheum*., 2009, **60**, 1895.
26 US Food and Drug Administration. Center for drug evaluation and research, Application number: 203214Orig1s000, Approval letter, https://www.accessdata.fda.gov/drugsatfda_docs/nda/2012/203214Orig1s000MedR.pdf, (Accessed September 2017).
27 H. Neubauer, A. Cumano, M. Müller, H. Wu, U. Huffstadt and K. Pfeffer, *Cell*, 1998, **93**, 397.
28 D. E. Levy and C. A. Loomis, *N. Engl. J. Med*., 2007, **357**, 1655.
29 S. O. Park, H. L. Wamsley, K. Bae, Z. Hu, X. Li, S.-w. Choe, W. B. Slayton, S. P. Oh, K.-U. Wagner and P. P. Sayeski, *PLoS One*, 2013, **8**, e59675.
30 A. Tefferi, *Blood*, 2012, **119**, 2721.
31 A. Pardanani, J. R. Gotlib, C. Jamieson, J. E. Cortes, M. Talpaz, R. M. Stone, M. H. Silverman, D. G. Gilliland, J. Shorr and A. Tefferi, *J. Clin. Oncol.*, 2011, **29**, 789.
32 R. J. Riese, S. Krishnaswami and J. Kremer, *Best Pract. Res. Clin. Rheumatol.*, 2010, **24**, 513.
33 European Medicines Agency. Refusal of the marketing authorisation for Xeljanz (tofacitinib), EMA/248755/2013, EMEA/H/C/002542, 25. April 2013, http://www.ema.europa.eu/docs/en_GB/document_library/Summary_of_opinion_-_Initial_authorisation/human/002542/WC500142485.pdf, (accessed September 2017).
34 B. W. Dymock, E. G. Yang, Y. Chu-Farseeva and L. Yao, *Future Med. Chem.*, 2014, **6**, 1439.
35 D. L. Boyle, K. Soma, J. Hodge, A. Kavanaugh, D. Mandel, P. Mease, R. Shurmur, A. K. Singhal, N. Wei, S. Rosengren, I. Kaplan, S. Krishnaswami, Z. Luo, J. Bradley and G. S. Firestein, *Ann. Rheum. Dis.*, 2015, **74**, 1311.
36 C. J. Menet, O. Mammoliti and M. López-Ramos, *Future Med. Chem.*, 2015, **7**, 203.
37 Menet, C. J. M.; Van Rompaey, L. J. C.; Fletcher, S.R.; Blanc, J.; Jouannigot, N.; Hodges, A. J.; Smits, K. K. PCT Int. Appl. WO 2010010190 A1, 2010.
38 J. Gras, *Drug. Future*, 2014, **39**, 547.
39 C. J. Menet, S. R. Fletcher, G. Van Lommen, R. Geney, J. Blanc, K. Smits, N. Jouannigot, P. Deprez, E. M. van der Aar, P. Clement-Lacroix, L. Lepescheux, R. Galien, B. Vayssiere, L. Nelles, T. Christophe, R. Brys, M. Uhring, F. Ciesielski and L. Van Rompaey, *J. Med. Chem.*, 2014, **57**, 9323.
40 L. Van Rompaey, R. Galien, E. M. van der Aar, P. Clement-Lacroix, L. Nelles, B. Smets, L. Lepescheux, T. Christophe, K. Conrath, N. Vandeghinste, B. Vayssiere, S. De Vos, S. Fletcher, R. Brys, G. van 't Klooster, J. H. M. Feyen and C. Menet, *J. Immunol.*, 2013, **191**, 3568.
41 P. Norman, *Expert Opin. Investig. Drugs*, 2014, **23**, 1067.
42 Filgotinib Versus Placebo in Adults With Active Rheumatoid Arthritis (RA) Who Have an Inadequate Response to Biologic Disease-modifying Anti-rheumatic Drug(s) (DMARDs) Treatment. (2016). Retrieved from http://clinicaltrials.gov (Identification No. NCT02873936).
43 Filgotinib Alone and in Combination With Methotrexate (MTX) in Adults With Moderately to Severely Active Rheumatoid Arthritis Who Are Naive to MTX Therapy. (2016). Retrieved from http://clinicaltrials.gov (Identification No. NCT02886728).
44 Filgotinib in Combination With Methotrexate in Adults With Moderately to Severely Active Rheumatoid Arthritis Who Have an Inadequate Response to Methotrexate. (2016). Retrieved from http://clinicaltrials.gov (Identification No. NCT02889796).
45 Galapagos NV. Risks related to product development, regulatory approval and commercialization, http://reports.glpg.com/annual-report-2016/en/risk-factors/product-development-regulatory-approval-and-commercialization.html, (accessed September 2017).
46 A Study Comparing ABT-494 to Placebo and to Adalimumab in Subjects With Rheumatoid Arthritis Who Are on a Stable Dose of Methotrexate and Who Have an Inadequate Response to Methotrexate (SELECT-COMPARE). (2015). Retrieved from http://clinicaltrials.gov (Identification No. NCT02629159)
47 A Study Comparing ABT-494 Monotherapy to Methotrexate (MTX) Monotherapy in Subjects With Rheumatoid Arthritis (RA) Who Have an Inadequate Response to MTX (SELECT-MONOTHERAPY). (2016). Retrieved from http://clinicaltrials.gov (Identification No. NCT02706951)
48 M. C. Genovese, J. S. Smolen, M. E. Weinblatt, G. R. Burmester, S. Meerwein, H. S. Camp, L. Wang, A. A. Othman, N. Khan, A. L. Pangan and S. Jungerwirth, *Clin. Exp. Rheumatol.*, 2016, **34**, 318.

View Article Online
DOI: 10.1039/C7MD00568G

49 J. A. Hodge, T. T. Kawabata, S. Krishnaswami, J. D. Clark, J. B. Telliez, M. E. Dowty, S. Menon, M. Lamba and S. Zwillich, *J. Mol. Biol.*, 2009, **387**, 219.
50 N. K. Williams, R. S. Bamert, O. Patel, C. Wang, P. M. Walden, A. F. Wilks, E. Fantino, J. Rossjohn and I. S. Lucet, *Xenobiotica*, 2001, **31**, 811.
51 Y. Kimura, S. Atarashi, K. Kawakami, K. Sato and I. Hayakawa, *J. Med. Chem.* 1994, **37**, 3344.
52 G. M. Morris, R. Huey, W. Lindstrom, M. F. Sanner, R. K. Belew, D. S. Goodsell and A. J. Olson, *J. Comput. Chem.*, 2009, **30**, 2785.
53 Department of Medicine SoM, Indiana University. P450 Drug Interaction Table, http://medicine.iupui.edu/clinpharm/ddis/main-table, (accessed September 2017).
54 K. W. Ward, L. M. Azzarano, C. A. Evans and B. R. Smith, *Xenobiotica*, 2004, **34**, 353.
55 D. D. Brand, K. A. Latham and E. F. Rosloniec, *Nat. Protoc.*, 2007, **2**, 1269.
56 P. E. Whiteley and S. A. Dalrymple, Models of Inflammation: Adjuvant-Induced Arthritis in the Rat, in *Current Protocols in Pharmacology*, ed. S. J. Enna, John Wiley & Sons, Inc., New York, 2001, Vol. 2, 5.5.1–5.5.5.
57 Eurofins, Protocol Guide – KinaseProfiler™ Service Assay Protocols v64, http://www.komabiotech.co.kr/pdf/kinaseprofiler_assay_protocol_guide_eurofins_v64.pdf, (accessed December 2017).
58 M. Chartier, T. Chénard, J. Barker and R. Najmanovich, *PeerJ*, 2013, **1**, e126.
59 Chondrex, Inc. Protocol for the Successful Induction of Collagen-Induced Arthritis (CIA) in Mice, 2017, https://www.chondrex.com/documents/Mouse%20CIA.pdf, (accessed September 2017).
60 Hooke Laboratories. CIA Induction in DBA/1 Mice, 2013, https://hookelabs.com/protocols/pdf/CIA%20Induction%20in%20DBA1%20Mice.pdf, (accessed September 2017).
61 K. C. Sohn, S. J. Kang, J. W. Kim, K. Y. Kim, S. K. Ku and Y. J. Lee, *Biomol. Ther.*, 2013, **21**, 290.

View Article Online
DOI: 10.1039/C7MD00568G

Design, synthesis and evaluation of (*R*)-3-(7-(*methyl(7H*-pyrrolo[2,3-*d*]pyrimidin-4-yl)amino)-5-azaspiro[2.4]heptan-5-yl)-3-oxopropanenitrile as a JAK1-selective inhibitor

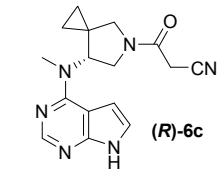

(*R*)-6c

JAK1 IC_{50} = 8.5 nM
JAK2 IC_{50} = 410 nM
Selectivity Index = 48

We discovered a new JAK1-selective inhibitor with the selective index of 48 and identified the efficacy in CIA and AIA models.